JOURNAL OF MATERIALS SCIENCE 26 (1991) 2150–2156

Mullite formation from xerogels of (0.84–2.2) $Al_2O_3 \cdot 1SiO_2$

FU-SU YEN, C. S. HSI, Y. H. CHANG
Department of Mineral and Petroleum Engineering, National Cheng Kung University, Tainan, Taiwan

H. Y. LU
Department of Material Engineering, Yet-Sun University, Kaohsung, Taiwan

Xerogels of (0.84–2.2) $Al_2O_3 \cdot 1SiO_2$ prepared by chemical coprecipitation of $Al(NO_3)_3 \cdot 9H_2O$ and $Si(OC_2H_5)_4$ experience three thermal reaction paths for mullite formation. Those with pseudoboehmite are found to form mullite via the paths of either Al–Si spinel → mullite transformation or γ-Al_2O_3 → θ-Al_2O_3 + amorphous SiO_2 → mullite, depending upon the ratios of Al_2O_3/SiO_2. Higher SiO_2 content may prefer the former reaction. Xerogels composed of bayerite form mullite via the route η-Al_2O_3 → γ-Al_2O_3 + amorphous SiO_2 → mullite. Mullite thus formed exhibits a different crystal size, being 20–25 nm for that obtained from pseudoboehmite and around 37 nm for bayerite. The highest yield of mullite formation may be achieved with xerogels of pseudoboehmite with the stoichiometric mullite compositions, $3Al_2O_3 \cdot SiO_2$.

1. Introduction

Ceramic powders of high purity and submicrometre size are of technological importance for attaining a fully-dense ceramic body with controlled microstructures and better physical properties.

Mullite is a characteristic constituent of traditional ceramics made from aluminosilicate. Mullite ceramics are of industrial interest due to their superior properties under high temperatures in mechanical stability, thermal shock resistance and infrared transparency. However, mullite powder of high purity and submicrometre size is difficult to synthesize using conventional methods. During the last decade various innovational chemical methods have been developed. These provide new ways of improving the homogeneous mixing of Al_2O_3 and SiO_2 in an aqueous system and controlling the impurities in the starting materials so as to obtain mullite powders with anticipated properties [1–4]. However, there are few reports concerning either the thermal behaviour of the Al_2O_3–SiO_2–H_2O (mullite) system or the influence of silicon hydroxide.

In the Al_2O_3–H_2O system, the crystalline phases are determined by the starting materials, the organic solvents, the additives and the reaction parameters [4–6]. Fibrous [7], non-fibrous and plate-like [4, 8] pseudoboehmites have been reported. On ageing in a mother liquor of pH > 7 with no alkali ions, pseudoboehmite will transform to somatoid bayerite [9]. In the synthesis of high purity mullite powders, the role of the crystalline phases formed in the xerogel is unclear. Hirata *et al.* [10] synthesized mullite powders from Al_2O_3–SiO_2 xerogels using aluminium and silicon alkoxides as starting materials. Nordstrandite, bayerite and boehmite gels were formed under different conditions. Hsi *et al.* [11] investigated the phase transformation during heating with a xerogel of mullite composition ($3Al_2O_3 \cdot 2SiO_2$) prepared from alkaline starting solutions. Two crystalline phases, pseudoboehmite and bayerite, were found to form. The former behaved as a single-phase xerogel [2] and the latter was diaphasic in nature [2] during the formation of mullite. The silica was in an amorphous state during the calcination.

This study examined the thermal reactions during formation of mullite from xerogels which had crystalline phases of pseudoboehmite and bayerite prepared from an alkaline starting solution of pH 8.3 and 10.4. Molar ratios of Al_2O_3/SiO_2 for the xerogels were 0.84:1 (Al-poor), 1.4:1 (stoichiometric mullite), and 2.2:1 (Al-rich). However, for bayerite, because similar results were obtained, only the $1.4Al_2O_3 : 1SiO_2$ composition will be discussed. The study places emphasis on the phase transformation of the major and minor phases during the route of mullite formation.

2. Experimental procedure

2.1. Starting materials and processing

Aluminium nitrate ($Al(NO_3)_3 \cdot 9H_2O$) and tetraethyl orthoxysilane (TEOS, $Si(OC_2H_5)_4$) were used as starting materials. They were mixed with three different $[Al^{3+}]/[Si^{4+}]$ ratios, 1.8, 3.3 and 4.8, each representing Al-poor, stoichiometric, and Al-rich precursors of mullite. The mixture was then dissolved in 75 ml ethyl

0022–2461/91 $03.00 + .12

alcohol (each mixture weighed about 135 g) as a starting solution. The solution was stirred for 1 h until optically homogeneous, and was then added to an agitated NH_4OH solution (reaction solution) over 1.5 h. The Al^{3+} and TEOS of the starting solution were hydrolysed and formed a colloidal suspension. The reaction solution contained 0.65 and 4.28 N NH_4OH. The selected reaction temperature was 25 °C. The colloidal solutions were aged for 6 h and filtrated on a Buchner funnel. The precipitates were cleaned by resuspending in distilled water and refiltrating; this was repeated three times. Dehydrolysis of the precipitates was carried out in a drying oven at 110 °C for 24 h and then the xerogels were obtained. The xerogels were ground into powders using an agate mortar and pestle.

2.2. Characterization

The gel powders were analysed using DTA at a heating rate of 10 °C min^{-1} to disclose the temperatures at which the exothermic/endothermic reaction occurred. These temperatures were adopted as references for the calcination of the gel powders, at a heating rate of 3.3 °C min^{-1} and soaking subsequently for 4 h. The specific surface area of the gel powders was determined using the BET method. Phase transformation during calcination was identified by X-ray diffraction (XRD) using CuK_α radiation and transmission electron microscopy (TEM) techniques. Quantitative analysis for mullite phase was performed by XRD using the standard method [12]. The relative diffraction intensities of mullite with respect to the internal standard, calcium difluoride, were obtained by scanning and evaluating the (1 1 1) peaks of mullite and CaF_2.

3. Results and discussion

3.1. Phase transformation during calcination

Table I lists the reaction conditions used in the preparation of the gels and the mineral phases presented under these conditions. It was found that the Al_2O_3/SiO_2 ratios of the gel are close to those of $[Al^{3+}]/[Si^{4+}]$ of the starting solution. Three samples represented gels of pseudoboehmite which were Al-poor (no. 1, Al_2O_3, 58.7 wt %, or $0.84Al_2O_3 \cdot SiO_2$), stoichiometric mullite (no. 2, 70.3%, or $2.8Al_2O_3 \cdot 2SiO_2$) and Al-rich (no. 3, 79.1%, or $2.2Al_2O_3 \cdot 1SiO_2$), and one of bayerite (no. 4, 70.3%, or $2.8Al_2O_3 \cdot 2SiO_2$). Mineral phases and the specific surface area of the gel powders are also inserted in Table I.

The DTA heating curves (Fig. 1) for the samples revealed that the gel powders underwent three endothermic reactions at about (i) 150 °C, (ii) 300 °C, and (iii) 500 °C, and two exothermic reactions at about (iv) 1000 °C and (v) 1270 °C. Sample 4 with bayerite

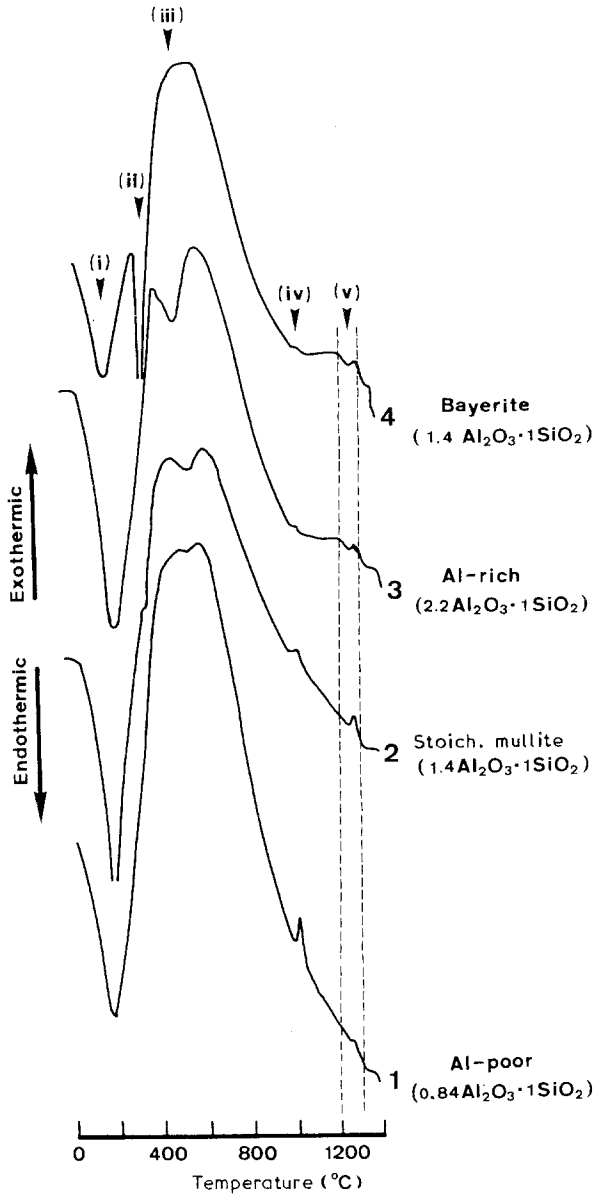

Figure 1 The DTA heating curves of gel powders.

TABLE I Sample preparation and properties of gels

Samples	Reaction conditions			Properties of gels			
	pH	T(° C)	Al^{3+}/Si^{4+}	$\frac{Al_2O_3}{Al_2O_3 + SiO_3}$ (wt %)	$(Al_2O_3:SiO_2)$[a]	BET ($m^2 g^{-1}$)	Phase[b]
1	8.3	25	1.8	58.7	(0.84:1)	337	PsB
2	8.3	25	3.3	70.7	(1.4 :1)	413	BsB
3	8.3	25	4.8	79.1	(2.2 :1)	370	PsB
4	10.4	25	3.3	70.4	(1.4 :1)	282	Ba(PsB)

[a] Mole ratio

[b] PsB, pseudoboehmite; Ba, bayerite; ( ) trace.

showed the highest peak of endotherm (ii). Endotherm (iii) become progressively smaller from sample 3, which had the highest Al_2O_3 content, to sample 1 which had the lowest Al_2O_3. The thermal behaviour during heating in the temperature range 950–1300 °C can be classified into two types: one for samples 3 and 4 and the other for samples 1 and 2.

Pseudoboehmite was of poor crystallinity, as can be seen from the diffused ring of the selected-area diffraction pattern (SADP), and appeared to be fibrillar in texture (Fig. 2a and b) for samples 1, 2 and 3, as reported previously [13, 14]. The bayerite (Fig. 3) was in the form of agglomerate-like particles of $-$ 700 nm size. The SADP revealed that some of the gel powder particles remained amorphous.

Because XRD identification (Table II) shows that bayerite disappeared while pseudoboehmite was retained after calcination at 300 °C, endotherm (ii) can be attributed to the decomposition of bayerite, beginning at a temperature lower than 300 °C [15, 16]

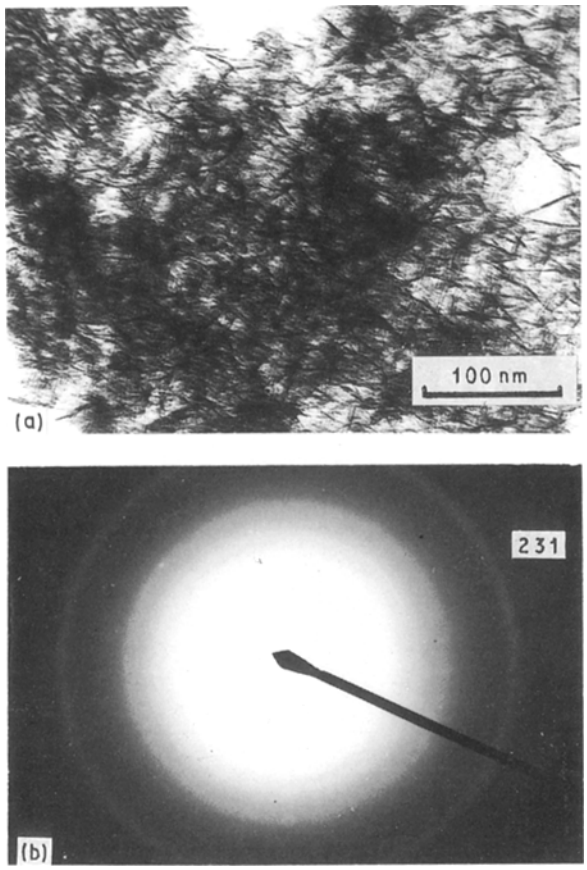

Figure 2 (a) Fibrillar textured pseudoboehmite and (b) its SADP. Sample 2.

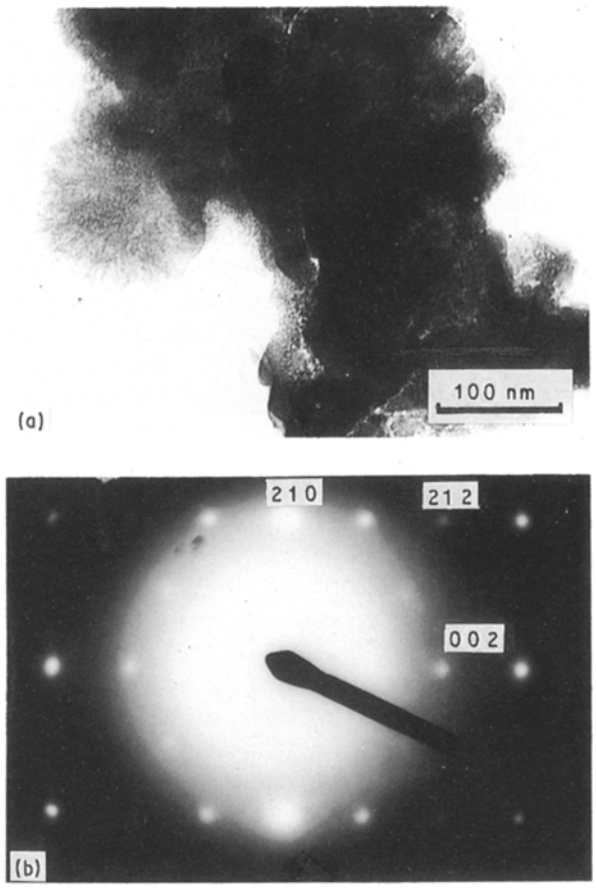

Figure 3 (a) Agglomerate-like bayerite and (b) its SADP, $Z = [1\bar{2}\bar{0}]$. Sample 4.

and leading to the formation of η-Al_2O_3. The η-Al_2O_3 was in a form of sericite-like agglomerated globes (Fig. 4a, b) and eventually achieved better crystallinity after calcining at 600 °C (Fig. 4c, d). However, the only trace amounts were found in samples 1, 2 and 3. Particles of η-Al_2O_3 coarsened to 300 nm and then transformed to θ-Al_2O_3 (Fig. 5) after the 1000 °C calcination which is comparable with the temperature range 850–1150 °C reported [15, 16].

For samples 1, 2, and 3, the sharpness of endotherm (iii) became progressively evident with increasing amount of pseudoboehmite present in the samples (Fig. 1, Table I). From examination of the phases obtained after annealing at 500 °C, it is seen that the endotherm represents the decomposition of pseudoboehmite to an amorphous phase, or the transformation of pseudoboehmite to γ-Al_2O_3 at $\sim$ 400–500 °C [9, 13, 17]. The SADP revealed that γ-Al_2O_3 had, in fact, been formed by annealing at temperatures lower than $\sim$ 350 °C for sample 2

TABLE II Major phases[a] of calcined Al_2O_3–SiO_2 gels (XRD and TEM)

Sample	Temperature (° C)					
	110	350	600	1000	1200	1300
1	PsB	A	A	S	SM	M
2	PsB	PsB	A	S	SM	M
3	PsB	PsB	γs	γ(S)	γM	(θ)M
4	(PsB)Ba	(PsB)η	η	θ	θ	(θ)M

[a] PsB, pseudoboehmite; Ba bayerite; a amorphous; η, η-Al_2O_3; θ, θ-Al_2O_3; γ, γ-Al_2O_3; S, Al–Si spinel; M. mullite; ( ) trace.

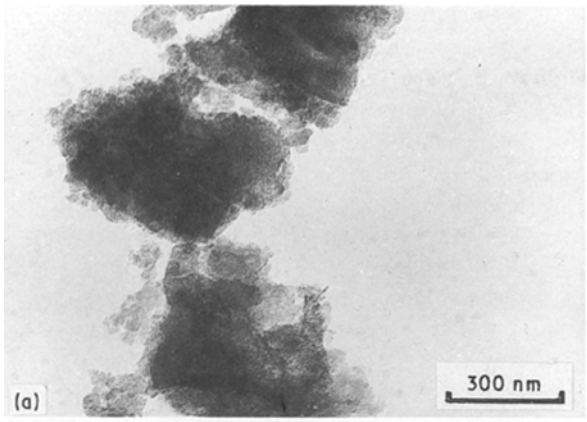

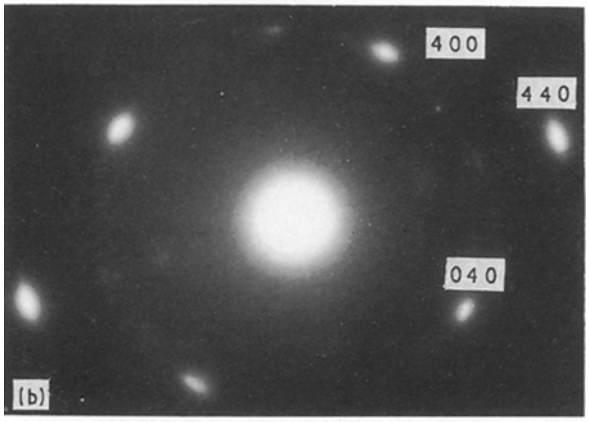

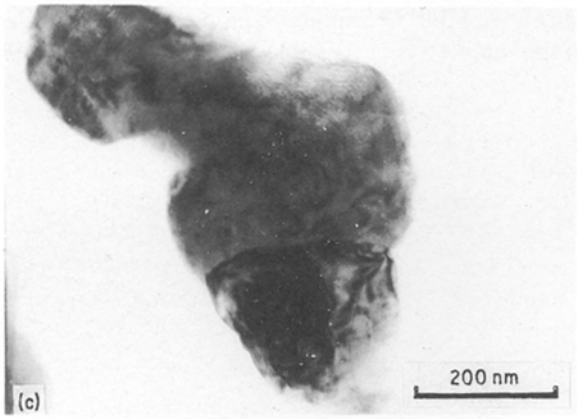

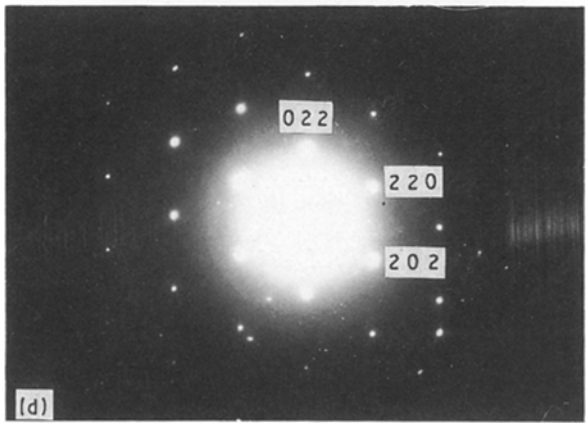

Figure 4 (a, b) η-Al_2O_3 particle from 300 °C calcination $Z = [0\,0\,1]$. Sample 4. (c, d) Better-crystallized η-Al_2O_3 from 600 °C calcination, $Z = [\bar{1}\,1\,2]$. Sample 4.

(Fig. 6). However, the decomposition of fibrillar pseudoboehmite and its transformation to γ-Al_2O_3 was not completed unless annealed at 600 °C for 4 h for the

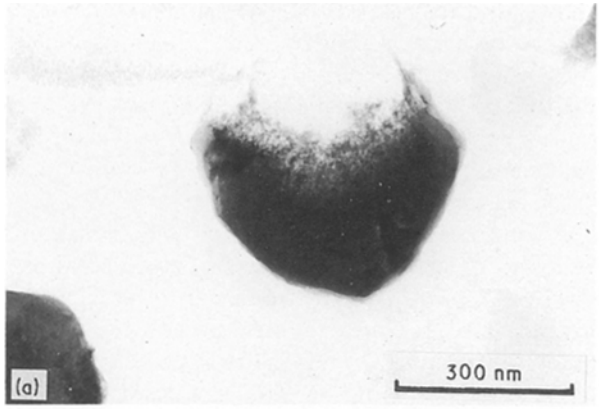

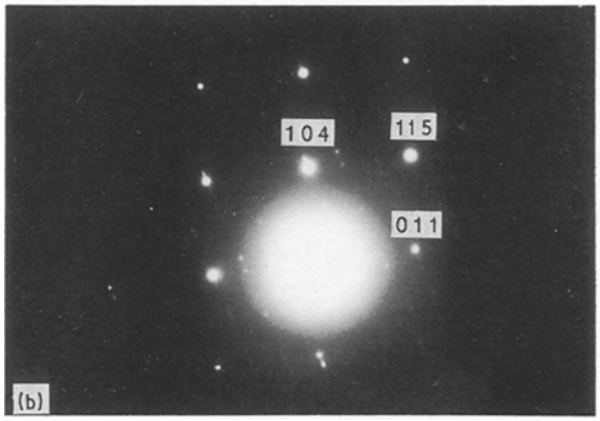

Figure 5 (a) θ-Al_2O_3 particles obtained from 1000 °C calcination, $Z = [4\,1\,\bar{1}]$, and (b) their SADP. Sample 4.

Al-rich xerogel of pseudoboehmite, sample 3 and could be formed as a minor phase in samples 1 and 2. This temperature is in good agreement with the range 400 °–700 °C reported by Iler [18] and Dwivedi and Gowda [19].

The spinel phase [20, 21] which appeared after calcining pseudoboehmite at 600 °C and existed as aggregates of fine particles (Fig. 7), became the only phase found in the samples 1 and 2 (after heating to 1000 °C), and occurred as a minor phase in sample 3 (Table II). It is noted that, although samples containing pseudoboehmite may behave similarly before endotherm (iii) took place, the transformed phases, after heating above 600 °C, may eventually be different as the Al_2O_3 content increased. For xerogels of Al-poor and stoichiometric mullite, the Al–Si spinel was predominant but for the Al-rich one the γ-Al_2O_3 eventually became the major phase (Table II).

3.3. Mullite formation

From the change in height of exotherm (iv) at $\sim$ 1000 °C, which became more manifest as the SiO_2 content of the samples increased, the pseudoboehmite xerogel may correspond to that in the rapid hydrolysis (RH) obtained by Okada and Otsuka [20]. However, in the presence of γ-Al_2O_3 instead of Al–Si spinel as a major phase in Al-rich xerogels, sample 3 experienced a phase transformation resembling that of a slow hydrolysis (SH), in which mullite and spinel occurred simultaneously [20] (Table II). These phenomena can

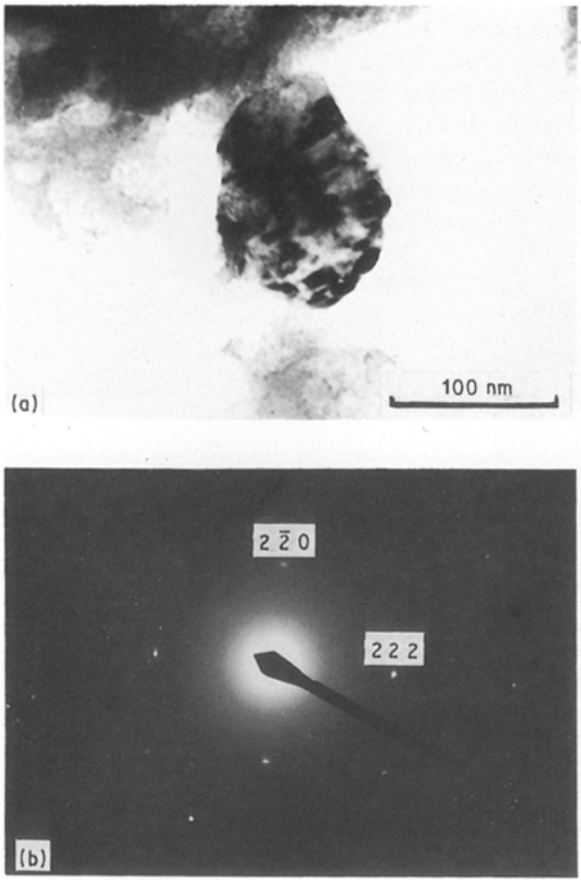

Figure 6 (a) γ-Al_2O_3 formed at a lower temperature of $\sim$ 300 °C, $Z = [\bar{1}\,1\,2]$. (b) The corresponding SADP. Sample 2.

be used to explain the exothermic reactions occurring between exotherms (iv) and (v). The formation of mullite [2, 3, 17] may result from (1) a monophase of the Al_2O_3–SiO_2 system in which the mullite was formed by transformation of Al–Si spinel, and (2) a diphasic Al_2O_3–SiO_2 system in which the θ-Al_2O_3, transformed from η-Al_2O_3 (sample 4) or from γ-Al_2O_3 (sample 3) reacted with amorphous SiO_2 to form mullite at about 1200 °C. These reactions continued over the temperature range $\sim$ 1150–1300 °C [2] (Fig. 1). Fig. 8 shows a mullite, about 400 nm in size, formed at 1300 °C as evinced from the SADP.

Following Hoffman's definition, all samples are a mixture of single-phase and diphasic xerogels [2, 3]. The xerogels of samples 1 and 2, however, are probably predominantly single-phase while that of samples 3 and 4 are diphasic. Three paths of mullite formation may occur in these samples during calcination. In sample 1, the single-phase xerogel yielded Al–Si spinel which was responsible for giving rise to exotherm (iv) [2, 3, 21]. The spinel was then transformed to mullite giving rise to exotherm (v) [17, 21]. Similar reasoning can be applied for sample 2, but because a relatively weak exotherm (iv) was observed, sample 2 may behave partially as a diphasic xerogel (Fig. 1, Table II).

In sample 4 the θ-Al_2O_3 which transformed from η-Al_2O_3 reacted with amorphous SiO_2 to form mullite above 1200 °C. Similar phenomena may take place in the sample 3 (Fig. 1, Table II). The barely detectable

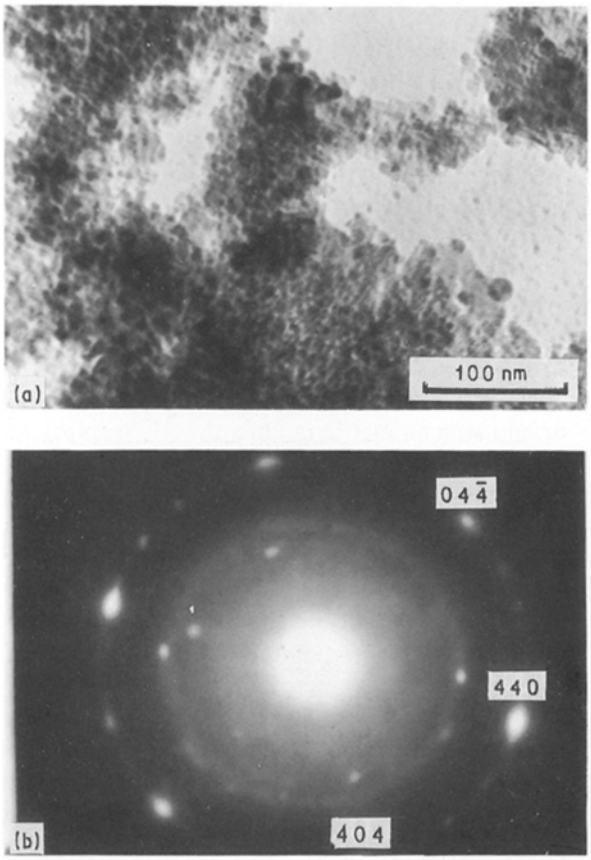

Figure 7 (a) Spinel from 600 °C calcination showing the formation of aggregates, $Z = [\bar{1}\,1\,1]$. (b) The corresponding SADP. Sample 2.

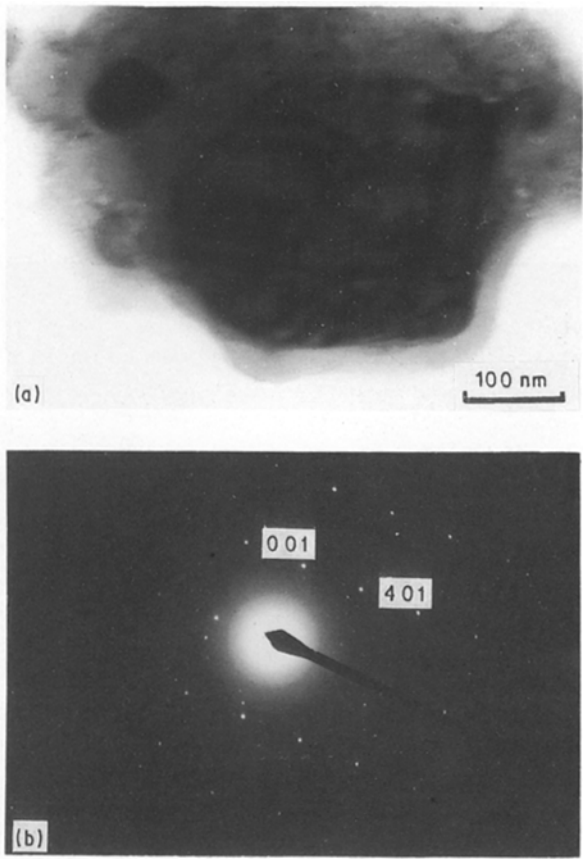

Figure 8 (a) Mullite crystal from 1300 °C calcination and (b) its SADP, $Z = [0\,1\,0]$. Sample 2.

exotherm (iv) and TEM examination revealed that Al–Si spinel coexisted with γ-Al_2O_3. Eventually the final transformation of the spinel to mullite occurred at about 1250 °C (DTA), which is believed to take place in samples 1 and 2. The γ-Al_2O_3 which first transformed to θ-Al_2O_3 above 1000 °C and then reacted with amorphous SiO_2 to form mullite at about 1200 °C, was comparable to that occurring in sample 4. Consequently the three formation paths of mullite can be summarized as follows.

1. Pseudoboehmite → Al–Si spinel → mullite
   (samples 1, 2 and minor part of 3)
2. Pseudoboehmite → γ-Al_2O_3 → θ-Al_2O_3 (+ amorphous SiO_2) → mullite
   (Major reaction in sample 3)
3. Bayerite → η-Al_2O_3 → θ-Al_2O_3 (+ amorphous SiO_2) → mullite
   (sample 4)

The exothermic reactions occurring in the temperature range 1250–1300 °C may then imply different meanings for different samples: it resulted mainly from the transformation of Al–Si spinel to mullite for samples 1 and 2 while it represented thermal reactions between θ-Al_2O_3 and amorphous SiO_2 to form mullite, for the samples 3 and 4. It is noted that the temperature of exotherm (v) shifted from 1260 °C to 1270 °C for samples 1 and 2 and from 1280 °C to 1300 °C for samples 3 and 4, possibly rising with increasing θ-Al_2O_3 content in the samples.

Al–Si spinel phase has been defined to be formed from Al_2O_3 and SiO_2 [8, 20]. For samples 1, 2 and 3 in which pseudoboehmite was the major phase, because their SiO_2 content decreased from sample 1 to 3 (or Al_2O_3 increased as the sequence goes up), the formation of Al–Si spinel would then decrease from sample 1 to sample 3 in this case. As a consequence, the trend in the formation of γ-Al_2O_3 and the subsequent transformation to θ-Al_2O_3 [6] increased from sample 1 to sample 3.

The temperature of the transformation to mullite does not seem to be related to the Al_2O_3 content of the sample. However, it can be closely related to good mixing of Al_2O_3 with SiO_2 in the gels [2, 20] as well as the replenishment of SiO_2 to the surface of the Al_2O_3 particles [6]. It is possible that a relatively higher degree of inhomogeneity in the mixture will be encountered if the amount of pseudoboehmite in the samples is increased. Mullite formation from diphasic xerogels involves the kinetic nucleation and growth [22]. Samples with lower SiO_2 contents certainly require an even higher ratio of participation from the only available SiO_2 constituent to react with Al_2O_3. Poor mixing of Al_2O_3–SiO_2 xerogels would bring about a need for a longer diffusion distance of the SiO_2 constituent to Al_2O_3 if no reactable Al_2O_3 existed in the vicinity of SiO_2. A higher temperature to achieve transformation to mullite seems to be necessary.

3.4. Particle size of mullite

Fig. 9 shows the relationships of the weight fraction of mullite yield with the related mullite crystal size formed at 1200, 1300 and 1400 °C annealing (see also Table III). Obviously the mullite crystals obtained by calcining samples containing pseudoboehmite possessed a similar crystal size, being 20–25 nm, and those from bayerite were ~ 37 nm. The difference can be attributed to the larger crystal size of the bayerite gel, as demonstrated by its specific surface area (Table I) as well as the formation mechanism. The growth of the mullite particles began after the number of nucleations and the yield rate had reached a maximum at about

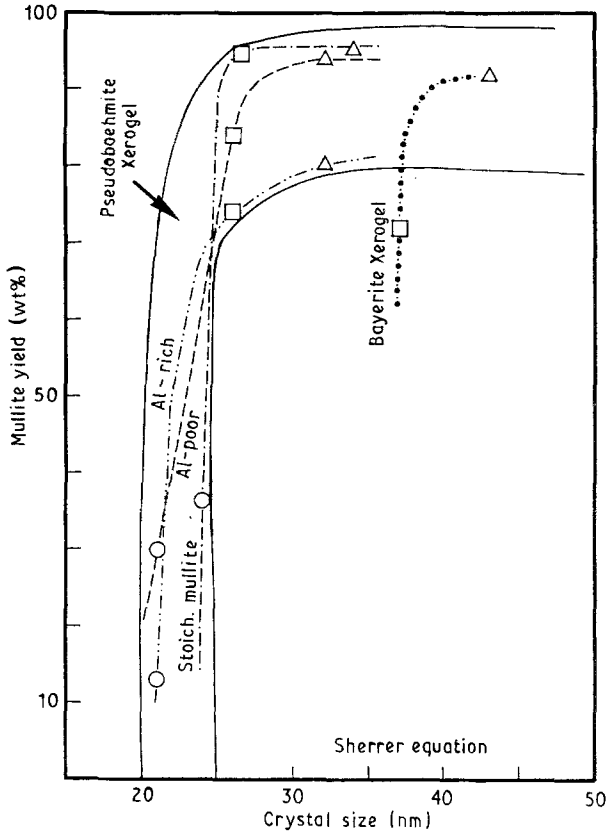

Figure 9 Relationships between the weight percentage of mullite yield and the crystal size, at (△) 1400 °C, (□) 1300 °C and (○) 1200 °C.

TABLE III Mullite formation and the related crystal size (d, from the Scherrer equation) at different calcining temperatures

	1200 °C		1300 °C		1400 °C	
	Mullite (%)	d (nm)	Mullite (%)	d (nm)	Mullite (%)	d (nm)
NMD-20	30	21	84	26	94	32
MA-20	36	24	95	29	95	34
NMA-20	13	21	74	26	81	32
MD-20	0	–	72	37	93	42

1300 °C. Obviously, growth resulted from the combination of small nuclei. The highest yield of mullite was obtained from xerogels with a stoichiometric mullite composition.

4. Conclusions

1. Al_2O_3–SiO_2 xerogels containing pseudoboehmite and bayerite show three thermal reaction paths for mullite formation.

Path A pseudoboehmite (Al-poor and stoichiometric mullite)
→ Al–Si spinel → mullite
Path B pseudoboehmite (Al-rich) → γ-Al_2O_3
→ θ-Al_2O_3 (+ SiO_2) → mullite
or → Al–Si spinel → mullite (path A)
Path C bayerite → η-Al_2O_3 → θ-Al_2O_3
(+ SiO_2) → mullite

2. Mullite formed from xerogels of pseudoboehmite will have smaller crystal size than that from bayerite, being 20–25 nm and 37 nm respectively, before crystal growth starts.

3. The highest yield of mullite was obtained from xerogels of pseudoboehmite–amorphous SiO_2 phases with a chemical composition near to the stoichiometric mullite composition.

References

1. S. PROCHAZKA and F. J. KLUG, *J. Amer. Ceram. Soc.* **66** (1983) 874.
2. D. W. HOFFMAN, R. ROY and S. KOMARNENI, *ibid.* **67** (1984) 468.
3. A. K. CHAKRAVORTY and G. H. GHOSH, *ibid.* **69** (1986) 202.
4. J. OSAKA, *Nature* **191** (1961) [4792] 1000–1.
5. S. KANZAKI, H. TABATA, T. KUMAZAWA and S. OHTA, *Amer. Ceram. Soc.* **68** (1985) 6.
6. S. M. JOHNSON and J. A. PASK, *Amer. Ceram. Soc. Bull.* **61** (1982) 838.
7. K. HAMANO, T. SATO and Z. NAKAGAWA, *Yogyo-Kyokai-Shi* **94** (1986) 122.
8. G. W. BRINDLEY and N. NAKAHIRA, *J. Amer. Ceram. Soc.* **42** (1956) 311.
9. K. WEFER and G. M. BELL, Alcoa Research Laboratory, Technical Report No. 19 (1972).
10. Y. HIRATA, H. MINIMIZONO and K. SHIMADA, *Yogyo-Kyokai-Shi* **93** (1985) 36.
11. C. S. HSI, H. Y. LU and F. S. YEN, *J. Amer. Ceram. Soc.*, **72** (1989) 2208–10.
12. B. D. CULLITY, "Elements of X-ray Diffraction", 2nd Edn (Addison-Wesley, Reading, MA, 1987).
13. F. W. DYNYS, M. LJUNGBERG and J. W. HALLORAN, *Mater. Res. Soc. Symp. Proc.* **32** (1984) 321.
14. R. LAMBER, *J. Mater. Sci. Lett.* **5** (1986) 177.
15. A. NISHIKAWA, "Technology of Monolithic Refractories" (Pillbrico, Japan, 1970).
16. W. H. GITZEN, "Alumina as a Ceramic Material" (American Ceramic Society, Columbus, OH, 1970).
17. P. A. BADKAR and J. E. BAILEY, *J. Mater. Sci.* **11** (1976) 1794.
18. R. K. ILER, *J. Amer. Ceram. Soc.* **44** (1961) 618.
19. R. K. DWIVEDI and G. GOWDA, *J. Mater. Sci. Lett.* **4** (1985) 331.
20. K. OKADA and N. OTSUKA, *J. Amer. Ceram. Soc.* **69** (1987) 652.
21. B. SONUPARLAK, M. SARIKAYA and I. A. AKSAY, *ibid.* **70** (1987) 837.
22. W. C. WEI and J. W. HALLORAN, *ibid.* **71** (1988) 166.

Received 25 October 1989
and accepted 6 June 1990